

517-43
111675
8-11

MAPPING HYDROTHERMALLY ALTERED ROCKS IN THE NORTHERN GRAPEVINE MOUNTAINS, NEVADA AND CALIFORNIA WITH THE AIRBORNE IMAGING SPECTROMETER

FRED A. KRUSE

Cooperative Institute for Research in Environmental Sciences (CIRES)
Center for the Study of Earth from Space (CSES)
University of Colorado, Boulder Colorado 80309

ABSTRACT

Seven flightlines of Airborne Imaging Spectrometer (AIS) data acquired during 1984, 1985, and 1986 were analyzed for an area of hydrothermally altered rocks in the northern Grapevine Mountains, Nevada and California. The data were reduced to reflectance relative to an average spectrum, and an automated procedure was used to produce a color coded image displaying absorption band information. Individual spectra were extracted from the AIS images to determine the detailed mineralogy.

Two alteration types were mapped based upon mineralogy identified using the AIS data. The primary alteration type is quartz-sericite-pyrite alteration which occurs in northwest-trending zones in quartz monzonite porphyry. The AIS data allow identification of sericite (muscovite) based upon a strong absorption feature near $2.21\mu\text{m}$ and weaker absorption features near 2.35 and $2.45\mu\text{m}$. The second alteration type occurs as a zone of argillic alteration associated with a granitic intrusion. Montmorillonite was identified in this zone based upon a weak to moderate absorption feature near $2.21\mu\text{m}$ and the absence of the two absorption features at longer wavelengths characteristic of sericite. Montmorillonite could be identified only where concentrations of sericite were low enough that the sericite spectrum did not mask the montmorillonite spectrum.

INTRODUCTION

Alteration mapping is a time consuming process that usually involves extensive field work, laboratory analysis of thin sections, and X-ray studies. Additionally, most conventional studies of hydrothermal alteration do not recognize weathering products of altered rocks and seek to characterize only the altered bedrock. The determination of the relationship of minerals formed by near-surface weathering of alteration minerals to the original alteration patterns is necessary to allow use of these secondary minerals to locate new orebodies. High spectral resolution remote sensing provides us with a tool to start determining these relationships. This study discusses techniques for processing Airborne Imaging Spectrometer (AIS) data, and presents results for a study area in the northern Grapevine Mountains, Nevada and California. A total of seven AIS flightlines were analyzed (Figure 1).

ORIGINAL PAGE IS
OF POOR QUALITY

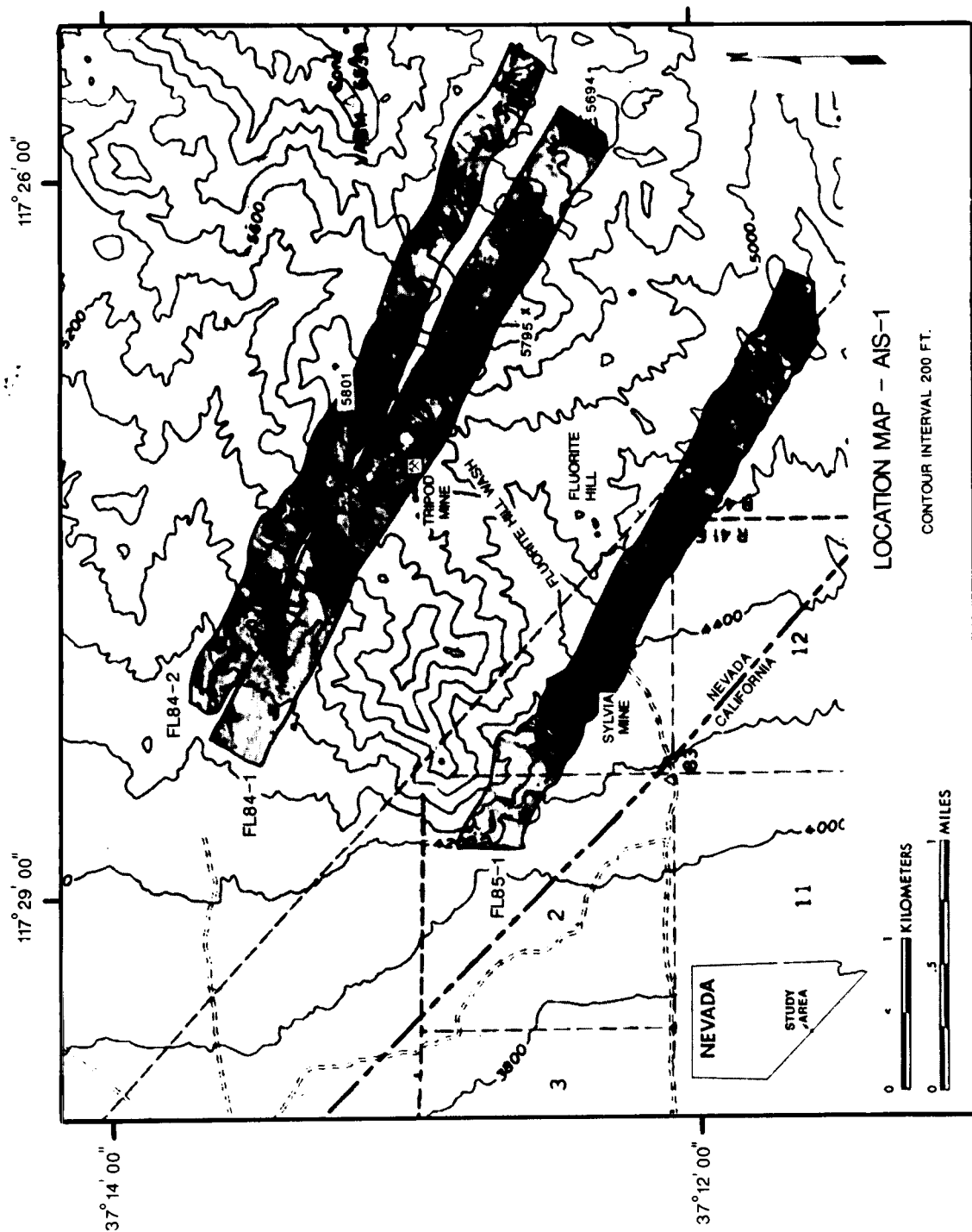
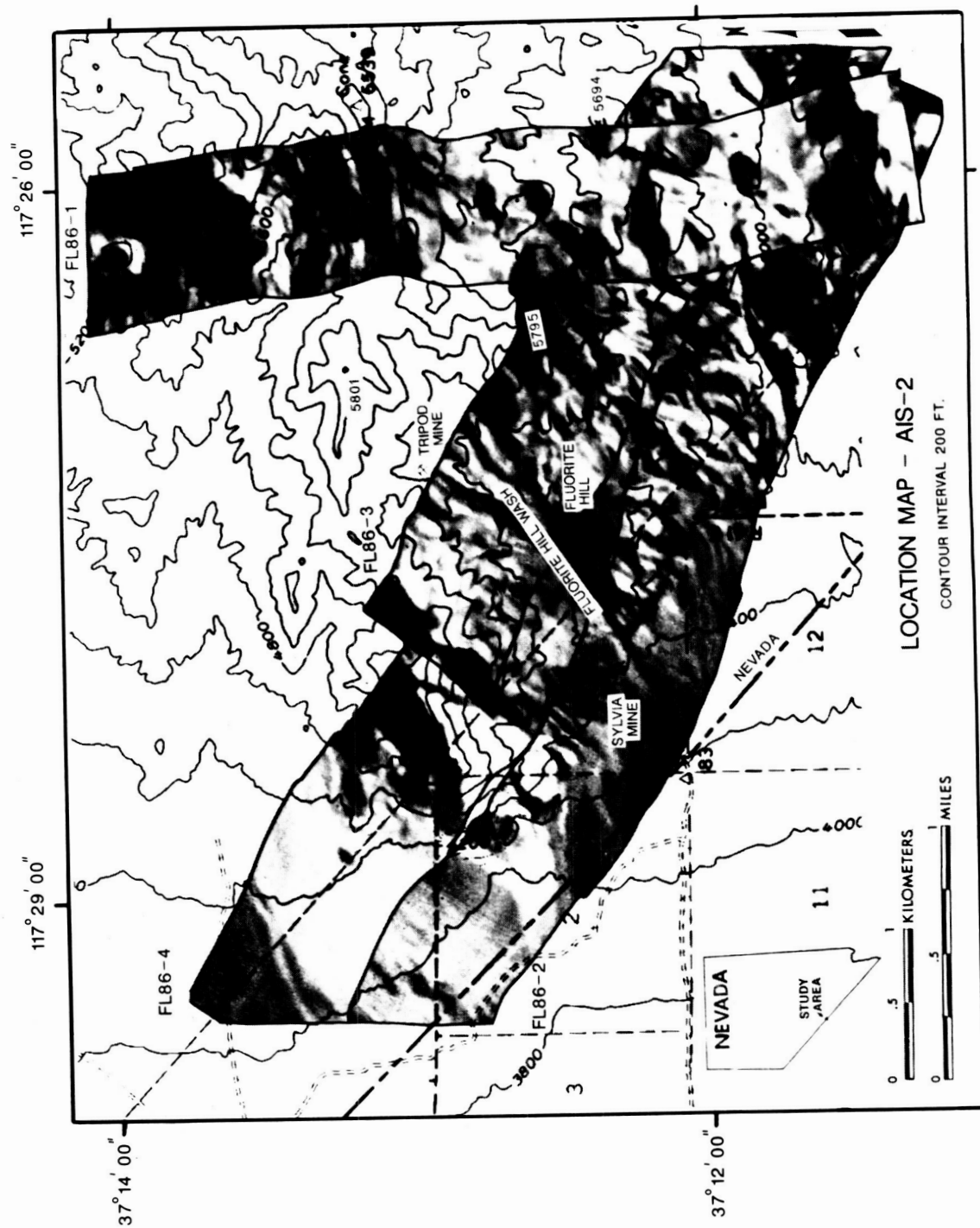


Figure 1a. 1984-85 AIS-1 flightline locations.



ORIGINAL PAGE IS
OF POOR QUALITY

Figure 1b. 1986 AIS-2 flightline locations.

The AIS is an experimental sensor designed to test two dimensional, near-infrared area array detectors. It images 32 (AIS-1, 1983-1985) or 64 (AIS-2, 1986) cross-track pixels simultaneously, collecting data in 128 contiguous narrow channels (AIS-1 [9.3nm], AIS-2 [10.6nm]) from approximately 1.2 to 2.5 μ m (Vane and others, 1983; Goetz and others, 1985; Vane, 1986). The area array detector is composed of a 32 X 32 element (AIS-1) or 64 x 64 element (AIS-2) HgCdTe detector sandwiched with a silicon charge-coupled device multiplexer (Rode and others, 1982; Wellman and others, 1983; Goetz and others, 1985). The spectrometer is stepped through four grating positions (AIS-1) or two grating positions (AIS-2) in the time it takes to advance one pixel on the ground to obtain the 128 spectral bands. The AIS-1 was flown on a NASA C-130 aircraft at an altitude of approximately 4,500 meters above mean terrain, resulting in an average ground pixel size of about 10.9 X 10.9 meters and a swath width of about 350 meters. The AIS-2 was flown at a similar altitude; but the revised instrument characteristics resulted in an average ground pixel of about 14.4 X 14.4 meters and swath width of about 920 meters.

The basic analysis approach for these data was to identify individual minerals using reflectance information, and to use mineral assemblages and distribution information to develop a better understanding of the weathered surfaces of the hydrothermally altered rocks. The research results are an example of the use of airborne spectroscopy for alteration mapping.

PREPROCESSING

Several preprocessing steps are required to prepare AIS data for analysis. Cosmetic processing is necessary to correct for dropped lines and vertical striping. Normalization is required to remove albedo effects. Individual bad lines (data drop outs) were removed by replacing the bad lines with the average of the two adjacent lines. Additionally, even though JPL had applied radiometric corrections to the data, a pronounced vertical striping pattern was still observed in the images, presumably caused by varying DC offsets in detectors in the pixel direction. The DC offsets were corrected using the procedures described by Dykstra and Segal (1985). Albedo differences were removed from the images using an "equal area normalization" as described in the Airborne Imaging Spectrometer Science Investigator's Guide (JPL, 1984, 1985). This allowed extraction of spectral information that had been masked by brightness variation.

Ideally the aircraft data should next be calibrated to absolute reflectance so that individual spectra can be compared directly with laboratory data for mineral identification. However, this requires a *priori* knowledge,

therefore, the approach taken was to use the properties of the data themselves to calculate an approximation of the reflectance. This approximation is defined here as "internal average relative (IAR) reflectance". IAR reflectance is calculated by determining an average spectrum for a single flightline or in this case for all flightlines acquired on an individual mission. Each spectrum (pixel with 128 channels) in the flightline is then divided by the average spectrum (Figure 2). The resulting spectra represent reflectance relative to the average spectrum and resemble laboratory spectra acquired of the same materials. One thing to remember when looking at an IAR reflectance spectrum, however, is that the average spectrum used to calculate the IAR reflectance spectrum may itself have spectral character related to mineral absorption features. This can adversely affect the appearance of the IAR reflectance spectra and limit their usefulness in comparisons with laboratory spectra. The average spectrum for the flightlines analyzed in this study did not contain any obvious mineral absorption features. The IAR reflectance technique has the added advantage of effectively removing the majority of atmospheric effects, since the average spectra contains contributions from the atmosphere, however, if the flight crosses an area that has wide variation in ground elevation, or the atmosphere is not uniform across the flight, the global average will not completely remove the effects of the atmosphere. A technique similar to the IAR reflectance procedure (logarithmic residuals) has been successfully demonstrated by Green and Craig (1985) and Huntington and others (1986).

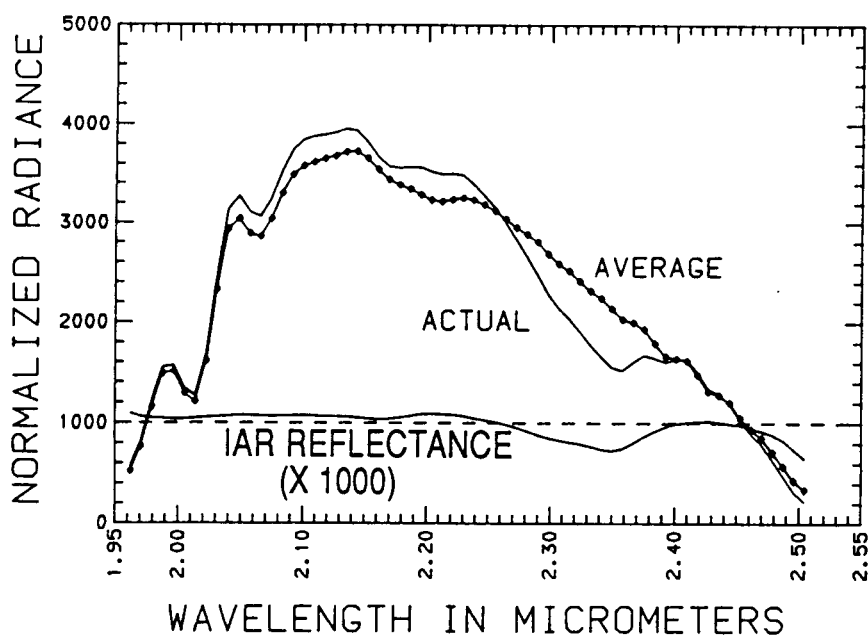


Figure 2. IAR Reflectance

DATA ANALYSIS

Once the IAR reflectance spectra are calculated then the data are ready for spectral analysis. Only the channels between 2.1 and 2.5 μ m were used for this analysis (the number of channels in this wavelength range varied between the 1984, 1985, and 1986 data sets). This region contains many of the characteristic absorption bands that allow mineralogical identification and generally avoids atmospheric absorption problems.

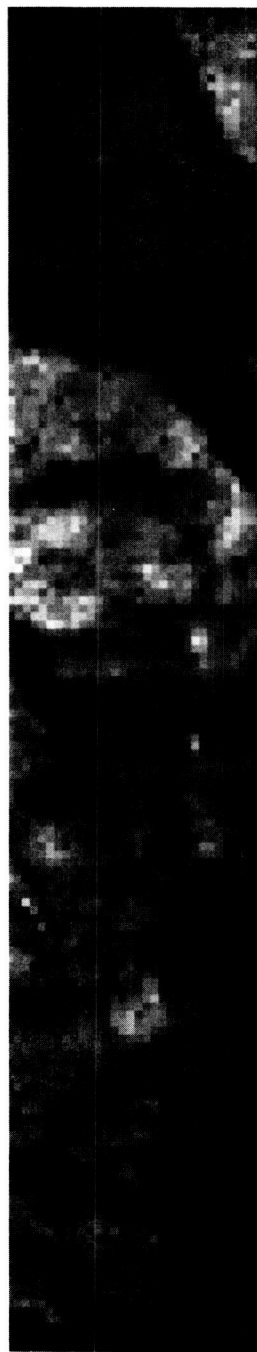
The image representation of IAR reflectance is shown in Figure 3. Dark areas in the IAR reflectance image (Figure 3B) represent absorption features. Color coded stacked spectra showing all of the spectra along a flightline (Marsh and McKeon, 1983; Kruse and others, 1985a, 1985b; Huntington and others, 1986) and a single-band color coded IAR reflectance image are shown in slide 5. A color coded spectrum (A) and the corresponding (idealized) spectral plot (B) show the relationship between the colors and the spectral features. The image on the left (C) consists of color-coded, stacked relative reflectance spectra. The x-axis represents the spectral direction (1.2 to 2.337 μ m), and the y-axis represents the flightline direction. Each line in the image represents a spectrum. The image on the right (D) is a color-coded single-band image for 2.21 μ m. The color bar in the upper right corner shows the colors for spectral features on both images. Black, purples and blues represent reflectance lower than the average spectrum (absorption features), green and yellow represent reflectance similar to the average, and oranges, reds, and whites represent reflectance higher than the average spectrum. The mineral absorption bands can be clearly seen in these images.

Algorithms were developed to identify automatically the strongest absorption feature in the 2.1 to 2.5 μ m portion of each AIS spectrum. Removal of a continuum (Clark and Roush, 1984) was used to place all of the spectra on a common reference plane (Figure 4). The continuum was calculated using a second order polynomial fitted to selected channels (channels without known absorption features) in the IAR reflectance spectra. The continuum was removed by dividing the polynomial function into the AIS data. The strongest absorption feature was defined as the wavelength position of the channel with the maximum depth from the continuum (Figure 5). Once the band position was identified, then the band depth and band width were calculated as the distance from the continuum at the band position, and the full width at one half the band depth respectively (Figure 5).

The next step was to put this information into a form that could be easily interpreted. The goal was to compress the spectral information into a single color-composite image representative of the data. This goal was accomplished using an intensity, hue, saturation (IHS) color transform (Raines, 1977; Raines and Knepper, 1983; Kruse and Raines, 1984) to map the three band parameters into red, green, blue (RGB)

ORIGINAL PAGE IS
OF POOR QUALITY

A.



B.



Figure 3. A. AIS-1 raw data - Dark areas represent dark rocks and shadows.
B. AIS IAR reflectance image - Dark areas represent absorption features at $2.21\mu\text{m}$.

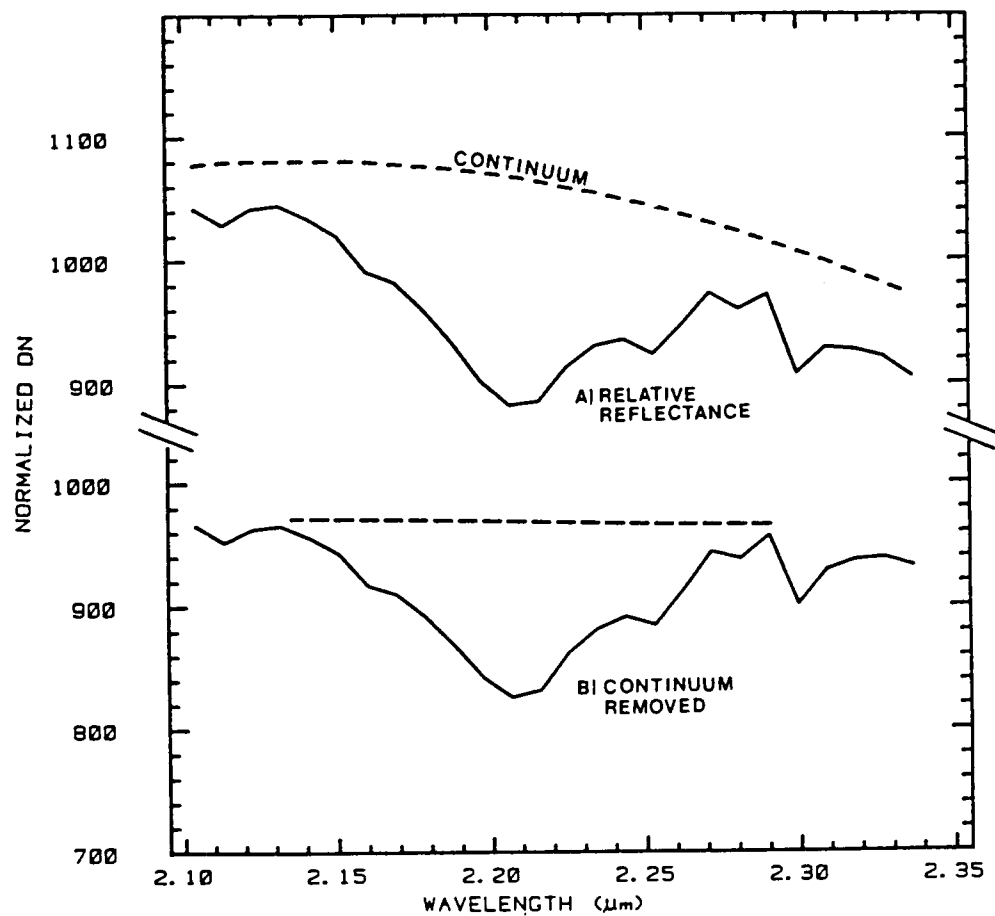


Figure 4. AIS continuum removal by division of 2nd order polynomial into each spectrum.

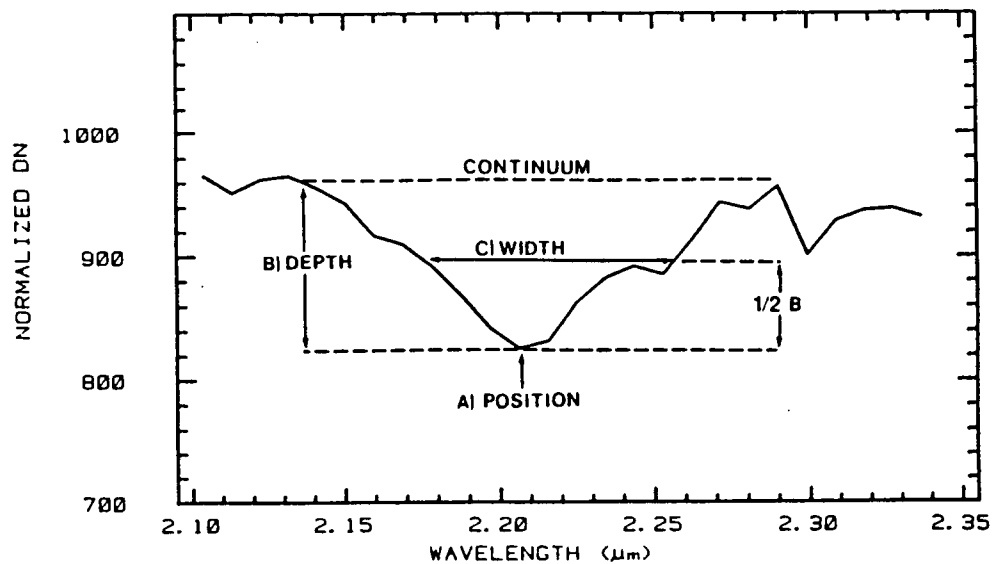


Figure 5. Absorption band parameters.

color space. The band position was mapped into hue, the band depth was mapped into intensity, and the band width was mapped into saturation. Transformation of the IHS encoded spectral information into the RGB color space produced an image in which all of the absorption band information for the strongest absorption feature between 2.1 and 2.4 μ m in each pixel was present in the color variation (Kruse and others, 1986; Kruse, 1987). This color variation was then mapped onto a single-band AIS image in which colored areas represent areas with absorption features deeper than a preselected cutoff value, and areas without absorption features are shown as the gray scale image (See slide 6). This type of image is here termed an "IHS-coded absorption band image."

RESULTS

Several minerals were identified. Sericite (muscovite) was identified by absorption features at 2.206, 2.346, and 2.445 μ m (Figure 6). Sericite must be identified using slightly different criteria in the three different AIS data sets (1984 AIS-1, 1985 AIS-1, 1986 AIS-2). In the 1984 data, the cutoff wavelength of 2.337 μ m prevents observation of the 2.346 and 2.445 μ m absorption features. However, the decreasing reflectance between 2.3 and 2.337 μ m is characteristic (Figure 6A). In the 1985 data, the cutoff wavelength of 2.4 μ m prevents observation of the 2.445 μ m absorption feature, however, the 2.346 μ m absorption feature is clearly seen (Figure 6A). The 1986 data include the necessary wavelength range to observe both the 2.345 and 2.445 absorption features, however, in many cases neither of these bands is fully resolved. Instead, a broad band is observed in the data covering the full range between about 2.3 and 2.48 μ m (Figure 6B).

Montmorillonite could be differentiated from sericite in the 1984 AIS-1 data based upon the characteristics of the 2.3 to 2.337 μ m portion of the spectra (Figure 7). Areas with sericite show decreasing reflectance in this region caused by the absorption feature near 2.35 μ m, while montmorillonite spectra remain fairly level in this region. No montmorillonite spectra were found in the 1985 or 1986 data. Spectra characteristic of montmorillonite were found in the 1984 data that covers an area of argillic/sericitic alteration. Areas of mixed montmorillonite and sericite could not be distinguished from those having only sericite because even small amounts of sericite mask the montmorillonite spectra.

Examination of the carbonate spectra from the 1984 data indicates that discrimination of calcite from dolomite is difficult because of the wavelength cutoff for that data set at approximately 2.34 μ m. The spectral range of the 1985 data extends to approximately 2.4 μ m and the 1986 data to 2.52 μ m, so these data do allow identification of calcite and dolomite (Figure 8) based on the presence of absorption features near

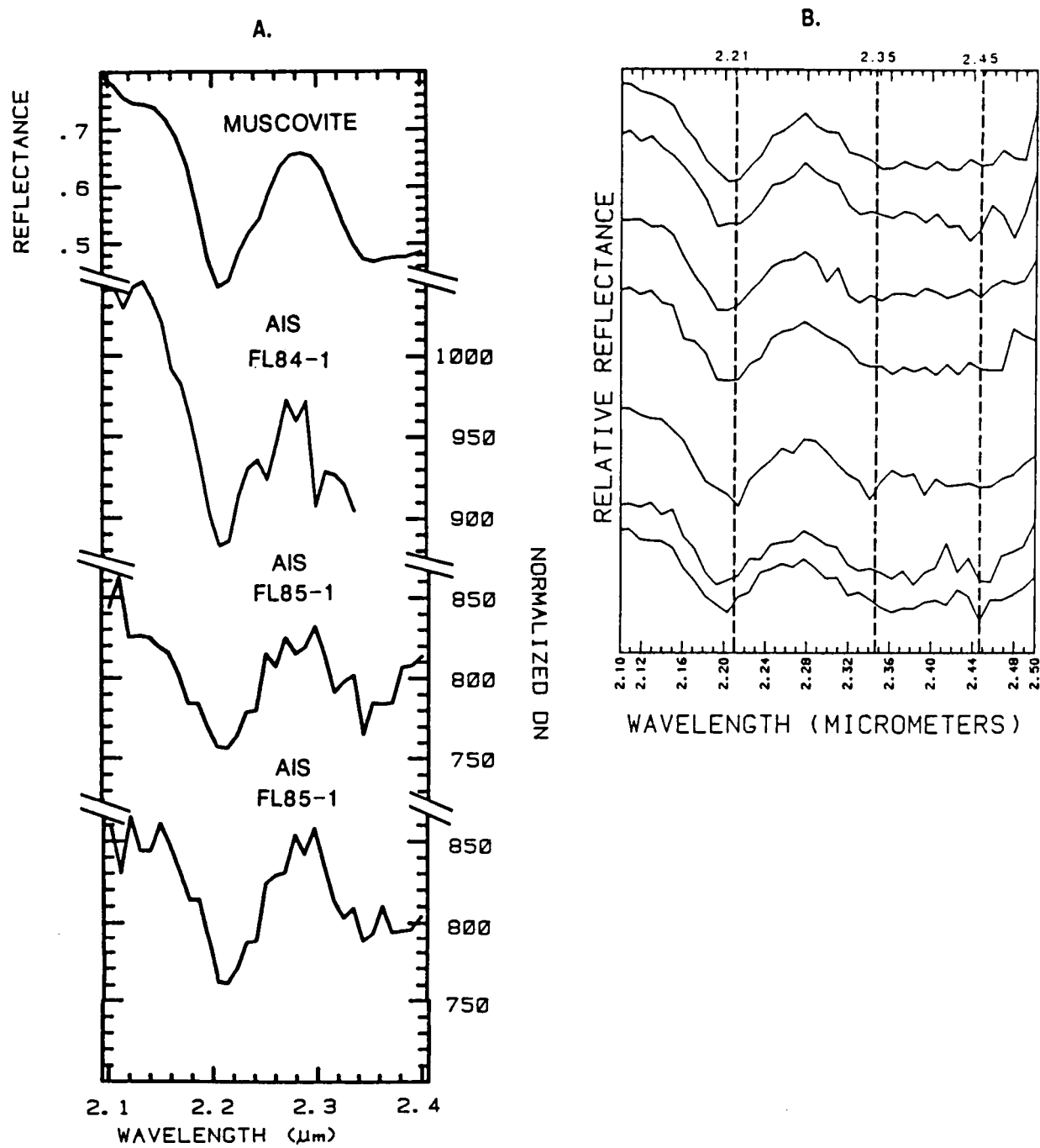


Figure 6. A. Laboratory spectrum for muscovite and AIS-1 spectra for sericite.
B. AIS-2 spectra for sericite.

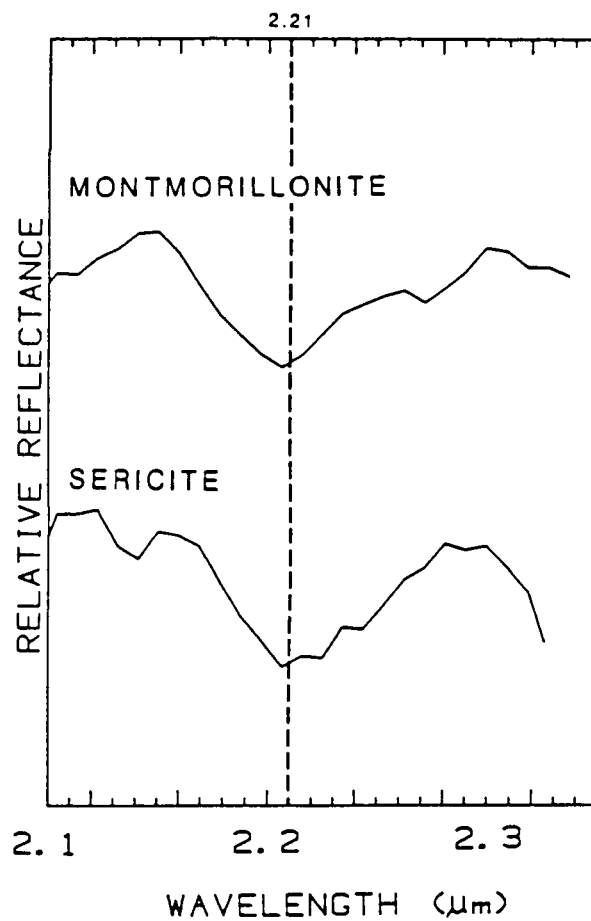


Figure 7. Comparison of AIS-1 spectra for montmorillonite and sericite.

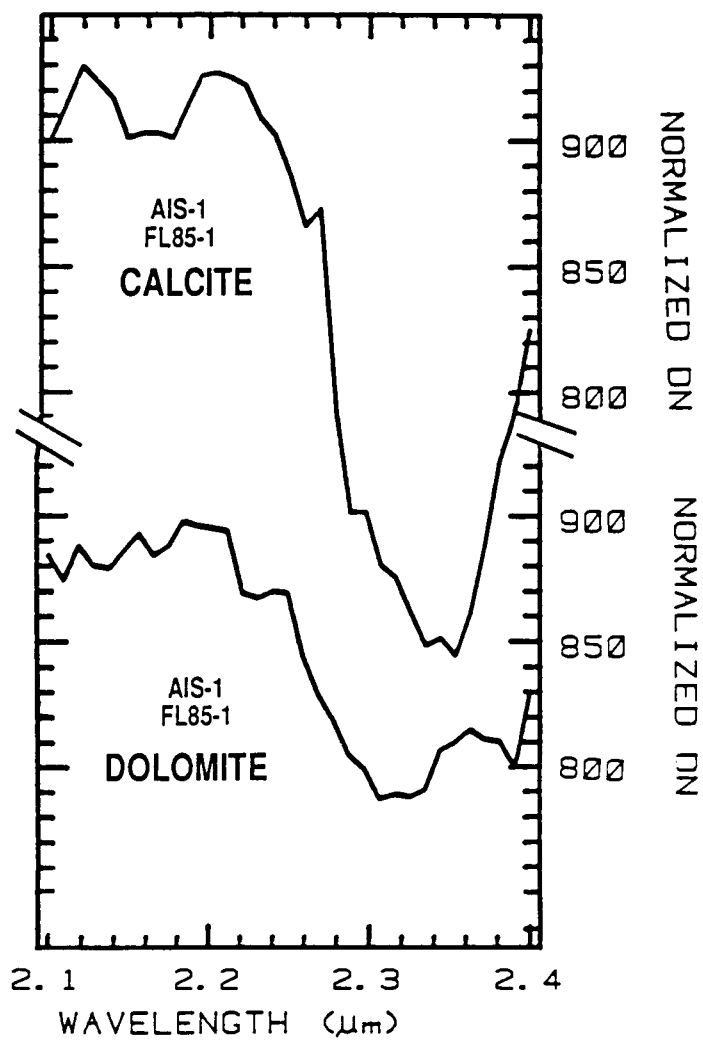


Figure 8. Comparison of AIS-1 spectra for calcite and dolomite.

2.34 and 2.32 μ m, respectively (Gaffey, 1984). For carbonate-derived alluvium the spectra have an absorption feature near 2.34 μ m, however, the feature is shallower and much broader.

Several spectra having some characteristics similar to epidote, tremolite, and actinolite were observed in the data. Low signal-to-noise ratios, however, precluded positive identification. The inability to precisely locate single pixels on the ground (and probable within pixel mixing) prevented independent confirmation of these minerals, although they are known to occur in the study area. Additionally, an unknown mineral with a broad absorption band near 2.43 μ m was observed in the volcanic rocks south of the study area (Figure 9). This area was not field checked and the mineral remains unidentified although the spectra somewhat resemble laboratory spectra of several zeolite minerals.

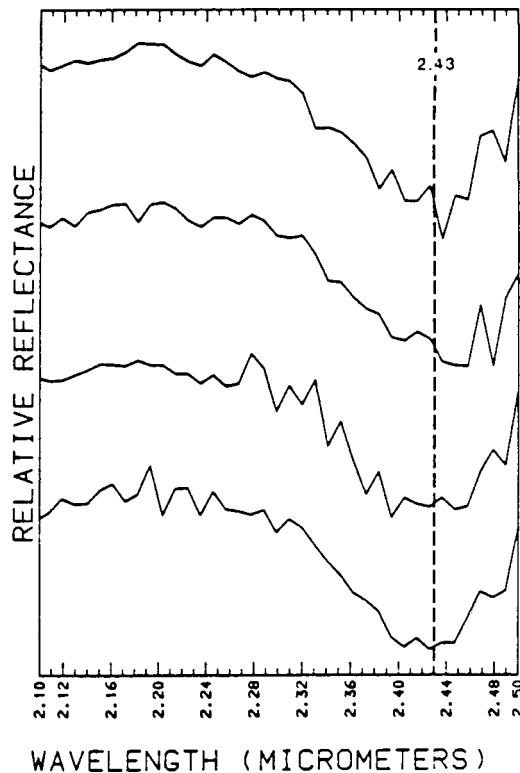


Figure 9. AIS-2 spectra of unknown mineral with broad absorption band near 2.43 μ m

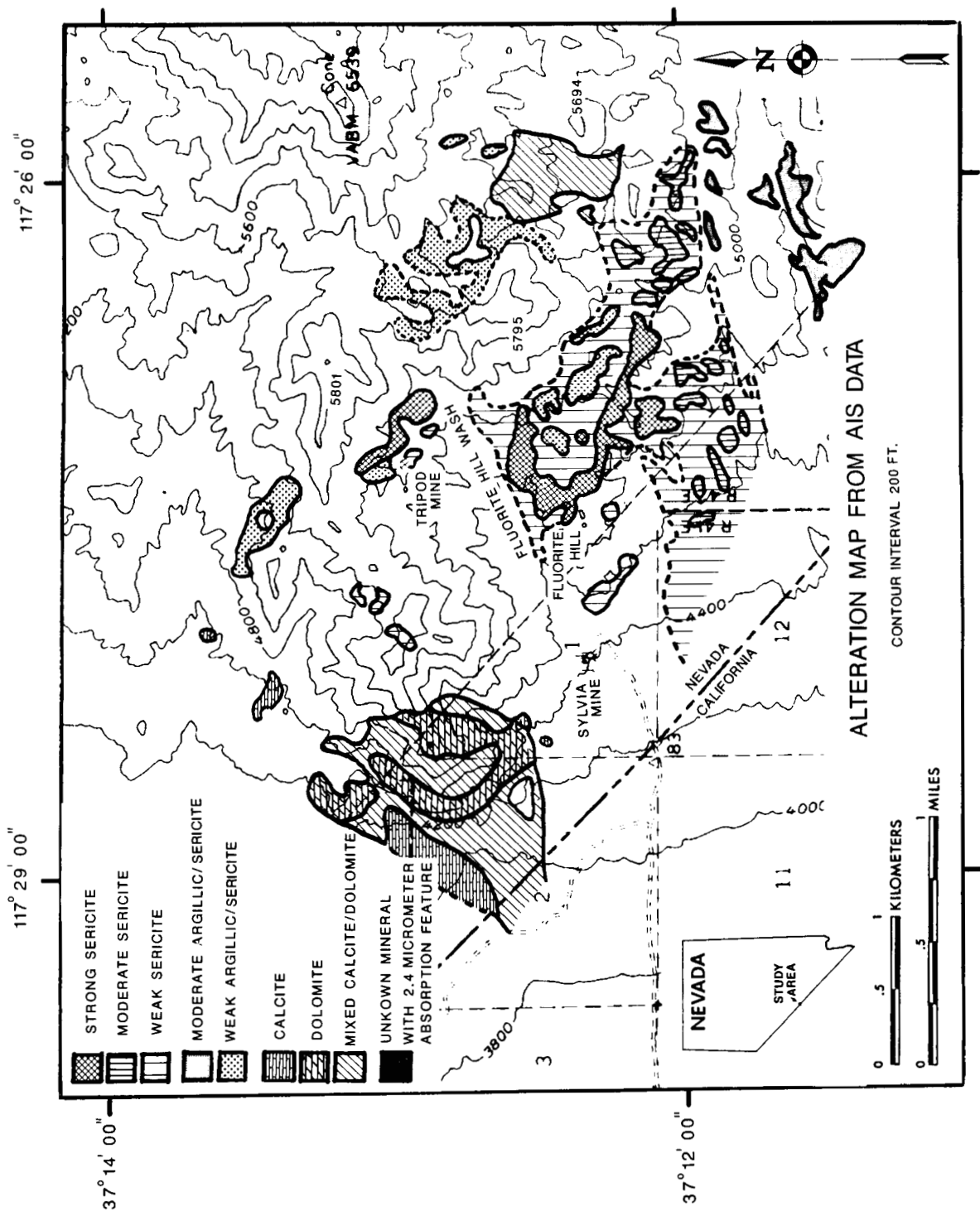
The absorption feature map and individual spectra were used to identify minerals and the color-coded density-sliced images and individual spectra were used to estimate alteration intensity based upon the strength of absorption features. Figure 10 gives a good picture of the alteration in the study area. The strongest alteration found using the AIS data is the northwest-trending zone of strong sericite alteration just southeast of Fluorite Hill. Additionally, the AIS data show that this zone of strong alteration is surrounded by an envelope of weak sericite alteration. The AIS alteration map also shows a zone of strong sericite alteration just northeast of the Tripod Mine.

The AIS data allow identification and mapping of carbonate minerals (Figure 10). Dolomite (yellow on slide 6) was mapped by an absorption feature near $2.32\mu\text{m}$ and calcite (reds on slide 6) was mapped by an absorption feature near $2.34\mu\text{m}$. The occurrence of spatially mixed calcite and dolomite pixels was mapped as mixed calcite and dolomite. Carbonate mineralogy generally was confirmed by X-ray diffraction within the limitations of sampling $\sim 15\text{m}$ pixels. Finer spatial resolution is required to resolve the individual limestone and dolomite beds.

The AIS alteration map (Figure 10) was field checked during 1986 and generally shows good correspondence with field mapping (Figure 11). The minerals mapped using the AIS data accurately represent the surface conditions mapped in the field and verified by petrological and X-ray diffraction studies. Both the field mapping and the mineralogical map produced from the AIS data show a linear, northwest-trending zone of strong sericitic alteration surrounded by a halo of weaker alteration. The AIS map is more detailed than the field map, particularly in areas of moderate to weak sericitic alteration, where the AIS map resolves very small areas of more intense alteration (south of Fluorite Hill) surrounded by a broader halo. During field mapping, these small areas were not mapped and the entire area was mapped as moderate sericitic alteration. In one area of weakly sericitized rock (VWS, Figure 11), X-ray diffraction analysis demonstrated that the predominant soil clay mineral is montmorillonite. Although this soil contains less sericite than montmorillonite, the spectral character of the sericite dominates the near-infrared spectra and montmorillonite was not identified using field, laboratory, or aircraft spectra; X-ray diffraction was required to identify the montmorillonite.

ACKNOWLEDGEMENTS

This research was conducted in partial fulfillment of the requirements of the Ph. D. degree at the Colorado School of Mines, Golden, Colorado. I would like especially to thank Dr. Keenan Lee (thesis advisor) who provided valuable guidance throughout the study. This work was funded in part by the U.S. Geological Survey, Denver, Colorado.



ORIGINAL PAGE IS
OF POOR QUALITY

Figure 10. Map of mineral distribution from the AIS data.

163

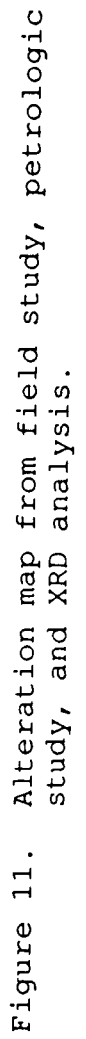


Figure 11. Alteration map from field study, petrologic study, and XRD analysis.

REFERENCES

- Clark, R. N., and Roush, T.L., 1984, Reflectance spectroscopy: Quantitative analysis techniques for remote sensing applications, Jour. Geoph. Res., v. 89, no. B7, p. 6329-6340.
- Dykstra, J. D., and Segal, D. B., 1985, Analysis of AIS data of the Recluse Oil Field, Recluse, Wyoming: in Proceedings, AIS workshop, 8-10 April, 1985, JPL Publication 85-41, Jet Propulsion Laboratory, Pasadena, California, p. 86-91.
- Gaffey, S. J., 1984, Spectral reflectance of carbonate minerals and rocks in the visible and near infrared (0.35 to 2.55 μ m) and its applications in carbonate petrology: Unpublished Ph. D. dissertation, University of Hawaii, 236 p.
- Goetz, A. F. H., Vane, Gregg, Solomon, J. E., and Rock, B. N., 1985, Imaging spectrometry for earth remote sensing: Science, v. 228, p. 1147-1153.
- Green, A. A., and Craig, M. D., 1985, Analysis of aircraft spectrometer data with logarithmic residuals: in Proceedings, AIS workshop, 8-10 April, 1985, JPL Publication 85-41, Jet Propulsion Laboratory, Pasadena, California, p. 111-119.
- Huntington, J.F., Green, A.A., and Craig, M. D., Preliminary Geological Investigation of AIS Data at Mary Kathleen, Queensland, Australia: in Proceedings, AIS workshop, 6-8 May, 1986, JPL Publication 86-35, Jet Propulsion Laboratory, Pasadena, California, p. 109-131.
- Jet Propulsion Laboratory, 1984, Airborne Imaging Spectrometer, Science Investigator's Guide to AIS DATA, Jet Propulsion Laboratory, Pasadena, California, 15 p.
- Jet Propulsion Laboratory, 1985, Airborne Imaging Spectrometer, Science Investigator's Guide to AIS DATA, Jet Propulsion Laboratory, Pasadena, California, 14 p.
- Kruse, F. A., 1987, Use of high spectral resolution remote sensing to characterize weathered surfaces of hydrothermally altered rocks: Ph. D. thesis (unpublished), Colorado School of Mines, Golden, 139 p.

- Kruse, F. A., Knepper, D. H., and Clark, R. N., 1986, Use of Digital Munsell Color Space to Assist Interpretation of Imaging Spectrometer Data -- Geologic Examples From the Northern Grapevine Mountains, California and Nevada: in Proceedings, AIS workshop, 6-8 May, 1986, JPL Publication 86-35, Jet Propulsion Laboratory, Pasadena, California, p. 132-137.
- Kruse, F. A., and Raines, G. R., 1984, A technique for enhancing digital color images by contrast stretching in Munsell color space: in Proceedings, International Symposium on Remote Sensing of Environment, Third Thematic Conference, "Remote Sensing for Exploration Geology", Colorado Springs, Colorado, 16-19 April, 1985, University of Michigan, Ann Arbor, p. 309-324.
- Kruse, F. A., Raines, G. L., and Watson, Kenneth, 1985a, Analytical techniques for extracting geologic information from multichannel airborne spectroradiometer and airborne imaging spectrometer data: in Proceedings, International Symposium on Remote Sensing of Environment, Fourth Thematic Conference, "Remote Sensing for Exploration Geology", San Francisco, California 1-4 April, 1985, Ann Arbor, Environmental Research Institute of Michigan, p. 309-324.
- Kruse, F. A., Raines, G. L., and Watson, Kenneth, 1985b, Analytical techniques for extracting mineralogical information from multichannel airborne imaging spectrometer data (Abs.): in Proceedings, AIS workshop, 8-10 April, 1985, JPL Publication 85-41, Jet Propulsion Laboratory, Pasadena, California, p. 105.
- Marsh, S. E., and McKeon, J. B., 1983, Integrated analysis of high-resolution field and airborne spectroradiometer data for alteration mapping: Econ. Geol., v. 78, no. 4, p. 618-632.
- Raines, G. R., 1977, Digital color analysis of color ratio composite Landsat scenes: in Proceedings, Eleventh International Symposium on Remote Sensing of Environment, University of Michigan, Ann Arbor, p. 1463-1472.
- Raines, G. R., and Knepper, D. H., Jr., 1983, A hue-saturation-intensity transform to improve hydrothermal alteration mapping: in International Geoscience and Remote Sensing Symposium Digest, 1983: Institute of Electrical and Electronic Engineers, v. 2, p. 1.1-1.3.
- Rode, J. P., Vural, K., Blackwell, J. D., Cox, F. A., and Lin, W. N., 1982, Characterization of a 32 X 32 HgCdTe focal plane: Proceedings of the IRIS Specialty Group on Infrared Detectors, San Diego, California.

- Vane, Gregg, 1986, Introduction to the Proceedings of the 2nd Airborne Imaging Spectrometer (AIS) Data Analysis Workshop: in Proceedings of the 2nd Airborne Imaging Spectrometer (AIS) Data Analysis Workshop, G. Vane and A.F.H. Goetz, editors, JPL Publication Number 86-35, Jet Propulsion Laboratory, Pasadena, California, p. 1-16.
- Vane, Gregg, Goetz, A. F. H., and Wellman, J. B., 1983, Airborne imaging spectrometer: A New Tool for Remote Sensing: IEEE Transactions on Geoscience and Remote Sensing, v. GE-22, no. 6, p. 546-549.
- Wellman, J. B., Goetz, A. F. H., Herring, M., and Vane, Gregg, 1983, An imaging spectrometer experiment for the shuttle: Proceedings 1983 International Geoscience and Remote Sensing Symposium (IGARS), IEEE cat No. 83CH1837-4.